The Nature of Chemical Interactions in Anhydrous Sodalites, $M_6(AlSiO_4)_6$, M = Na, Ag, Tl

Bo Brummerstedt Iversen,*,† Susan Latturner,‡ and Galen Stucky‡

Department of Chemistry, University of Aarhus, DK-8000 Århus C, Denmark, and Department of Chemistry, University of California, Santa Barbara, California 93106

Received May 17, 1999. Revised Manuscript Received July 28, 1999

Maximum entropy method (MEM) charge density analysis has been carried out on synchrotron X-ray powder diffraction data of a series of anhydrous sodalites, $M_6(AlSiO_4)_6$, M = Na, Ag, Tl. Analysis of the MEM electron densities reveals the nature of the interactions in the structures. The sodium atoms are bonded to the framework with predominantly electrostatic closed shell interactions, whereas the heavy metal ions form partly covalent bonds to the framework oxygens. At the same time the heavy metal atoms appear almost neutral, while the sodiums, as expected, are positively charged. The differences in the atomic charges and in the chemical interactions between the guest atoms and the framework are used to explain the varying dynamical behavior of the guest atoms. The guest−host interactions have pronounced effects on the framework atoms with Al, especially, showing reduced density. The removal of electron density from the framework bonds upon formation of covalent guest−host bonds is the cause of the abnormal chemical shifts and quadrupole coupling constants found in NMR for the heavy metal compounds. The fact that experimental electron densities can be estimated from powder diffraction data gives promise for increasing the understanding of the chemical and physical properties of a wide range of technologically important materials.

1. Introduction

Structural information on zeolite systems is of large technological importance because of their widespread use as catalysts, molecular sieves, and ion exchangers and for gas separation. However, to control the physical and chemical properties of zeolites, it is necessary to have a detailed understanding of not only the structure, but also the chemical interactions taking place between the framework atoms and the nonframework species trapped in the zeolite cavities. These interactions determine the chemical reactivity and dynamical behavior of the guest species. Conventionally the interactions between the framework and the guest species suspended in the cavities are thought to be mainly electrostatic in origin due to the presumed formal charges.[1] Unfortunately most experimental evidence regarding the nature of the interactions is indirect in the form of bond lengths determined from X-ray or neutron diffraction crystal structure analysis, NMR chemical shifts and coupling constants, or IR frequencies. Such indirect information has proven valuable in practice, but it would nevertheless be desirable if direct evidence could be obtained for example through analysis of the electron density distributions of the systems.[2] This is difficult since quantum mechanical calculations on extended inorganic structures still are relatively limited, although considerable advances have appeared in recent years.[3] In the case of anhydrous sodium sodalite, $Na_6(AlSiO_4)_6$, two studies have recently reported first principles density functional theory calculations.[4] These calculations yield unit cell axes lengths of 8.83[4a] and 9.29 Å,[4b] respectively, compared to 9.122 Å found experimentally.[5] Such discrepancies are chemically significant, and considering that a large portion of the sodalite literature is concerned with rationalization of chemical and physical behavior based on detailed structural comparisons, it seems some caution still should be exercised when interpreting theoretical results. A few studies have been carried out on systems where good single crystals are available,[6] which allow for X-ray charge densities to be determined by multipole modeling methods.[7] Downs and Swope examined the naturally occurring borosilicate danburite ($CaB_2Si_2O_8$) based on accurate single-crystal

* Corresponding author. Email: bo@kemi.aau.dk. Phone: +45 8942 3880. Fax: +45 8619 6199.

† University of Aarhus.

‡ University of California.

(1) (a) Sauer, J. *Chem. Rev.* **1989**, *89*, 199. (b) Blake, N. P.; Srdanov, V. I.; Stucky, G. D.; Metiu, H. *J. Phys. Chem.* **1995**, *99*, 2127.

(2) Bader, R. F. W. *Atoms in Molecules. A Quantum Theory*; Oxford University Press: Oxford, 1990.

(3) (a) Sauer, J. *Nature* **1993**, *363*, 493. (b) Shah, R.; Payne, M. C.; Lee, M. H.; Gale, J. D. *Science* **1996**, *271*, 1395. (c) Thomson, K. T.; Wentzcovitch, R. M.; Bukowinski, M. S. T. *Science* **1996**, *274*, 1880. (d) Wentzcovitch, R. M.; Martins, J. L.; Price, G. D. *Phys. Rev. Lett.* **1993**, *70*, 3947. (e) Nicholas, J. B.; Hess, A. C. *J. Am. Chem. Soc.* **1994**, *116*, 5428.

(4) (a) Filippone, F.; Buda, F.; Iarlori, S.; Moratti, G.; Porta, P. *J. Phys. Chem.* **1995**, *99*, 12883. (b) Thomson, K. T.; Wentzcovitch, R. M. *J. Chem. Phys.* **1998**, *108*, 8584.

(5) Felsche, J.; Luger, S.; Baerlocher, C. *Zeolites* **1986**, *6*, 367.

(6) (a) Downs, J. W.; Swope, R. J. *J. Phys. Chem.* **1992**, *96*, 4834. (b) Ghermani, N. E.; Lecomte, C.; Dusausoy, Y. *Phys. Rev. B* **1996**, *53*, 5231. (c) Kuntzinger, S.; Ghermani, N. E.; Dusausoy, Y.; Lecomte, C. *Acta Crystallogr. Sect B* **1998**, *54*, 819. (d) Ivanov, Y. V.; Belokoneva, E. L.; Protas, J.; Hansen, N. K.; Tsirelson, V. G. *Acta Crystallogr. Sect B* **1998**, *54*, 774.

(7) (a) Stewart, R. F. *J. Chem. Phys.* **1973**, *58*, 1668. (b) Hansen, N. K.; Coppens, P. *Acta Crystallogr. Sect A* **1978**, *34*, 909.

10.1021/cm9910658 CCC: $18.00
Published on Web 09/18/1999

X-ray diffraction data.[6a] They derived an analytical multipole representation of the electron density (ED) which they analyzed with the topological methods developed by Bader and co-workers.[2] In danburite the cations (Ca^{2+}) are bound to framework oxygens at distances ranging from 2.4008(11) to 2.4998(9) Å, which is 0.0−0.1 Å larger than the sum of ionic radii (0.99 + 1.32 Å). The values of the static electron density at the Ca−O bond critical points (ρ_c) ranged from 0.142(3) to 0.184(5) e/Å^3 and the Laplacian ($\nabla^2\rho_c$) values ranged from 3.23 to 4.14 e/Å^5. These values are indicative of bonds that are predominantly ionic, and indeed examination of the Laplacian function revealed the interaction to be closed shell like.[2] Ghermani and co-workers have studied natrolite and scolecite on the basis of accurate single-crystal diffraction data, which they used to model the electron density distribution.[6b,c] Their analyses also showed that the zeolite guest species (Na^+, Ca^{2+}, and H_2O) are bonded to the framework through electrostatic interactions. Unfortunately the majority of technologically important porous materials, while being crystalline, only give solids in the form of powders. However, recent advances in the analysis of diffraction data with the maximum entropy method (MEM) now allows estimation of charge distributions from powder diffraction data.[8] Even though MEM charge distributions determined from powder data are less accurate than from single-crystal data, the method nevertheless has a potential for providing new insights about the nature of guest−host interactions in porous materials.

The sodalites have been extensively investigated due to potential applications such as information storage based on regular arrays of cavities in which organized assemblies of specific clusters can be confined.[9] Besides their technological importance the aluminosilicate sodalites of general composition $M_{6+y}(AlSiO_4)_6(X)_y \cdot nH_2O$ also form excellent model compounds for more complicated framework structures. The framework, which consists of alternating, corner-sharing SiO_4 and AlO_4 tetrahedra, is a space-filling assembly of β-cages which have the shape of truncated octahedra (Figure 1). To compensate for the formal negative charge of the host framework, each cage contains a net positively charged collection of cations (M^+), anions (X^-), and water molecules. Depending on the exact nature of the cage-filling ions and water molecules, the framework can adjust itself in the form of a unit cell volume change.[10] The geometric distortions are thought to depend on the nature of the interactions between the nonframework ions with the framework as well as on the interactions between the nonframework species themselves.

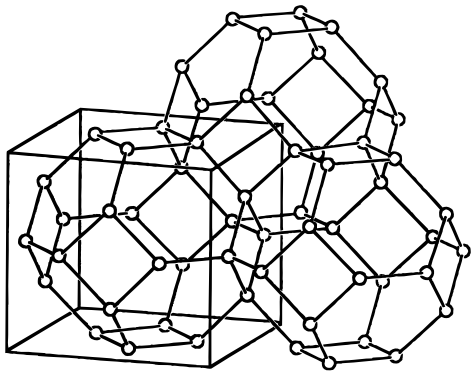

Figure 1. Schematic drawing of the sodalite framework. The circles correspond to regularly alternating aluminum and silicon atoms bridged by an oxygen atom. The metal atoms are located at the centers of hexagonal rings, but displaced along [111] toward the center of the cage.

To obtain information about guest−host interactions in porous materials, we have studied a series of anhydrous sodalites with the composition $M_6[AlSiO_4]_6$, M = Na, Ag, Tl, in the following named NS, AS, and TS, respectively. We have previuously reported the synthetic procedures for obtaining these compounds as well as their structural characterization with FTIR, solid-state NMR, and synchrotron powder diffraction.[11] The structural and spectroscopic data indirectly suggested that covalent bonding takes place between the heavy metal cations and the framework oxygens, whereas the interactions seemed to be mainly electrostatic for the alkali system. Here we present a further analysis of the synchrotron powder diffraction data using the MEM.[8] Using this procedure, we derive experimental electron density distributions of the structures, and analysis of these provides a direct characterization of the chemical interactions in the structure.

2. Experimental Section

2.1. Rietveld Refinement. In our related paper we presented details about the synthesis as well as experimental details about the synchrotron radiation data on AS and TS.[11] Both structures have static disorder of three metal atoms over four cubic positions (special position 8e in space group $P\bar{4}3n$), which result in pseudo-cubic diffraction patterns even at low temperatures (100 K). NS on the other hand goes through a phase-transition at 520 K, due to ordering of the metals atoms. The detailed aspects of this ordering will be reported elsewhere.[12] Here we are concerned with comparing the guest−host interactions for the different cations, and we therefore concentrate on the high-temperature dynamically disordered pseudo-cubic structure of NS. For all three systems the data were analyzed with the Rietveld method[11] using isotropic thermal parameters on all atoms to avoid absorbing possible uncorrected systematic errors into the structural parameters,

(8) (a) Takata, M.; Umeda B.; Nishibori, E.; Sakata, M.; Saito, Y.; Ohno, M.; Shinohara, H. *Nature* **1995**, *377*, 46. (b) Takata, M.; Nishibori, E.; Umeda, B.; Sakata, M.; Yamamoto, E.; Shinohara, H. *Phys. Rev. Lett.* **1997**, *78*, 3330.

(9) (a) Stein, A.; Macdonald, P. M.; Ozin, G. A.; Stucky, G. D. *J. Phys. Chem.* **1990**, *94*, 6943. (b) Stein, A.; Ozin, G. A.; Stucky, G. D. *J. Am. Chem. Soc.* **1990**, *112*, 904. (c) Stein, A.; Ozin, G. A.; Macdonald, P. M.; Stucky, G. D.; Jelinek, R. *J. Am. Chem. Soc.* **1992**, *114*, 5171. (d) Stein, A.; Ozin, G. A.; Stucky, G. D. *J. Am. Chem. Soc.* **1992**, *114*, 8119. (e) Wiebcke, M.; Engelhardt, G.; Felsche, J.; Kempa, P. B.; Sieger, P.; Schefer, J.; Fischer, P. *J. Phys. Chem.* **1992**, *96*, 392. (f) Wiebcke, M.; Sieger, P.; Felsche, Engelhardt, G.; Behrens, P.; Schefer, J. *Z. Anorg. Allg. Chem.* **1993**, *619*, 1321. (g) Engelhardt, G.; Felsche, J.; Sieger, P. *J. Am. Chem. Soc.* **1992**, *114*, 1173. (h) Nenoff, T. M.; Harrison, W. T. A.; Gier, T. E.; Keder, N. L.; Zaremba, C. M.; Srdanov, V. I.; Nicol, J. M.; Stucky, G. D. *Inorg. Chem.* **1994**, *33*, 2472.

(10) (a) Pauling, L. *Z. Kristallogr.* **1930**, *74*, 213. (b) Depmeier, W. *Acta Crystallogr., Sect. B* **1984**, *40*, 185. (c) Depmeier, W. *Z. Kristallogr.* **1992**, *199*, 75. (c) Hassan, I.; Grundy, H. D. *Acta Crystallogr Sect B* **1984**, *40*, 6. (d) Behrens, P.; Kempa, P. B.; Assmann, S.; Wiebcke, M.; Felsche, J. *J. Solid State Chem.* **1995**, *115*, 55. (e) Hu, X.; Depmeier, W. *Z. Kristallogr.* **1992**, *201*, 99. (f) Depmeier, W. *Acta Crystallogr. Sect B* **1988**, *44*, 201. (g) Depmeier, W.; Buhrer, W. *Acta Crystallogr. Sect B* **1991**, *47*, 197. (h) Depmeier, W.; Melzer, R.; Hu, X. *Acta Crystallogr. Sect B* **1993**, *49*, 483.

(11) Latturner, S.; Sachleben, J.; Iversen, B. B.; Hanson, J.; Stucky, G. D. *J. Phys. Chem. B* **1999**, *103*, in press.

(12) Cambell, B.; Iversen, B. B.; Delgado, J. M.; Blake, N.; Shannon, S. R.; Latturner, S.; Hanson, J.; Cox, D.; Stucky, G. D.; A. K. Cheetham, A. K. In preparation.

Table 1. Summary of Experimental Details

	$Na_6[AlSiO_4]_6$ (NS)	$Ag_6[AlSiO_4]_6$ (AS)	$Tl_6[AlSiO_4]_6$ (TS)
radiation	synchrotron	synchrotron	synchrotron
T (K)	673	100	100
wavelength (Å)	0.9341	0.9341	0.9341
μ_1 (cm^{-1})	12.4	85.7	421.9
sample container	1 mm capillary	1 mm capillary	1 mm capillary
exposure time (min)	11	60	60
step scan increment (deg)	0.02	0.01	0.01
space group	$P\bar{4}3n$	$P\bar{4}3n$	$P\bar{4}3n$
a (Å)	9.1683(1)	9.1189(1)	8.9653(1)
pattern range (deg)	6−54	6−54	6−54
no. of observations	2400	4697	4748
no. of structural parameters	8	8	8
no. of profile parameters	8	8	10
no. of background parameters	16	20	18
Rwp	0.034	0.042	0.017
Rp	0.025	0.032	0.010
GoF	4.13	4.96	2.06
R_F	0.058	0.015	0.029
R_F(MEM)	0.036	0.020	0.019

Table 2. Selected Interatomic Distances (Å) and Angles (deg)

	$Na_6[AlSiO_4]_6$	$Ag_6[AlSiO_4]_6$	$Tl_6[AlSiO_4]_6$
Si−O	1.605(5)	1.63(1)	1.72(5)
Al−O	1.709(5)	1.71(1)	1.65(4)
M−O	2.582(6)	2.3350(3)	2.635(5)
	2.700(7)	2.953(3)	3.225(4)
M−M			
intracage	6.07(1)	6.240(3)	3.734(2)
intercage	4.601(1)	4.5641(1)	5.1851(8)
M−(0,0,0)	3.74(1)	3.821(2)	2.2863(9)
O−Si−O	107.4(1) (×4)	108.8(1) (×4)	108.6(4) (×4)
	113.6(2) (×2)	110.8(2) (×2)	111.2(7) (×2)
O−Al−O	108.2(1) (×4)	109.33(9) (×4)	108.1(4) (×4)
	112.2(2) (×2)	109.8(2) (×2)	112.3(8) (×2)
Al−O− Si	156.3(2)	149.0(4)	139.6(3)
O−M−O	116.9(2)	119.70(2)	91.1(2)

and thereby biasing the MEM densities. A summary of refinement residuals and crystallographic parameters are given in Table 1, and important interatomic distances and angles are listed in Table 2. On the basis of the Rietveld model, structure factors were extracted on an absolute scale from the powder diffraction patterns. These structure factors were used as input for MEM calculations. As can be seen in Table 2, the Al−O and Si−O bond lengths in TS are opposite to what is normally found in aluminosilicate framework structures. For all the structures the Rietveld refinements were carried without any restraints on the parameters. If we restrain the Al−O bond lengths to 1.7 Å and the Si−O bond lengths to 1.6 Å in the refinement of TS, a slight increase in R factor is observed. The interchanged bond lengths could either be real due to the strong interaction between Tl and the framework, or be a minor flaw in the refinement caused by the presence of very heavy atoms next to the oxygen. However, the estimated standard uncertainties (su) on the bond lengths show that the differences to the conventional values are not significant. More importantly the use of restraints in the refinement has no effect on the extracted structure factors from the observed data. Since the present study focuses on MEM densities rather than structural refinement we list the unconstrained values.

2.2. MEM Calculations. The MEM has been extensively tested in charge density reconstructions during the past decade.[13] Furthermore a project under the International Union of Crystallography is currently scrutinizing the method.[14] Compared to conventional least-squares optimization, the MEM uses the full Bayes equation, and includes an entropy term in the optimization besides the χ^2 function.[15] In the approximation introduced by Collins[16] and implemented in the MEED program[13b] from Nagoya University, Japan, the MEM ED is calculated on a grid using an iterative procedure in which the density in pixel x of the unit cell is given as

$$\rho_x = \exp\left(\ln \tau_x + F_0\lambda/N\sum ((F_{\mathbf{H}}^{obs} - F_{\mathbf{H}}^{cal})/\sigma_{\mathbf{H}})^2 \exp(2\pi i\mathbf{H}x)\right) \quad (1)$$

In this formula $\mathbf{H}$ is a lattice vector and x is the pixel position in the unit cell. F_0 is the number of electrons in the unit cell, λ is a Lagrangian multiplier, and N is the number of observed structure factors. $F_{\mathbf{H}}^{obs}$ are the experimentally observed structure factors, $F_{\mathbf{H}}^{cal}$ are the calculated structure factors obtained as the Fourier summation of the unit cell density, and $\sigma_{\mathbf{H}}$ is the su of structure factor $F_{\mathbf{H}}^{obs}$. τ_x is a prior density which may contain information about the system from other sources. In normal applications of the MEM the iterations are stopped when the constraint function, χ^2, has reached a value of 1. In the present study we have carried out the MEM calculations using 64 × 64 × 64 pixel grids with uniform prior distributions. In all cases, it was found that use of structure factor su's calculated by the GSAS program did not give convergence even when applying previously established weighting schemes based on the length of the lattice vector.[17] We therefore introduced new su's based on the difference between $F_{\mathbf{H}}^{obs}$ and $F_{\mathbf{H}}^{cal}$ after the Rietveld refinement. The values of $\Delta F_{\mathbf{H}} = F_{\mathbf{H}}^{obs} - F_{\mathbf{H}}^{calc}$ gives an indication of how well a given structure factor has been estimated by the Rietveld model, and in the ideal refinement this difference should on average equal the su. With these $\sigma(F_{\mathbf{H}}^{obs})$ values convergence was quickly obtained for all the structures. The corresponding densities had very low crystallographic R factors (Table 1) and were virtually free of spurious ghost features in the low density regions. It should be pointed out that MEM densities obtained from powder diffraction data inherently are less accurate and contain less detail, than single-crystal MEM densities. Furthermore it is well-known that MEM densities contain slight method dependent bias,[13d,f] as well as small unphysical ghost features.[13g] In general optimizations with uniform priors give more spurious features than optimization carried out with well chosen nonuniform priors.[13f] For accurate single-crystal data, it has also been shown that the reliability of the MEM densities can be increased by performing valence electron optimizations rather than all-electron optimizations.[13f] However, in the present study we are primarily concerned with qualitative trends of density features having substantial magnitude. Thus, the conclusions we draw are highly unlikely to be affected by the specific MEM method used. Furthermore the conclusions are unchanged even if very large errors are assigned to the densities (1−2 e/Å^3 in the bonding regions).

3. Results and Discussion

3.1. Guest−Host Interactions. In the anhydrous sodalites the M−O bond lengths suggest a difference in guest−host interactions between the alkali and the

(13) (a) Sakata, M.; Sato, M. *Acta Crystallogr. Sect A* **1990**, *46*, 263. (b) Kumazawa, S. Kubota, Y.; Takata, M.; Sakata, M.; Ishibashi, Y. *J. Appl. Crystallogr.* **1993**, *26*, 453. (c) Iversen, B. B.; Larsen, F. K.; Souhassou, M.; Takata, M. *Acta Crystallogr. Sect. B* **1995** , *51*, 580. (d) Iversen, B. B.; Jensen, J. L.; Danielsen, J. *Acta Crystallogr. Sect. A* **1997**, *53*, 376. (e) Vries, R. Y.; Briels, W. J.; Feil, D. *Phys. Rev. Lett.* **1996**, *7*, 1719. (f) Roversi, P.; Irwin, J. J.; Bricogne, G. *Acta Crystallogr. Sect. A* **1998**, *54*, 971. (g) Jauch, W.; Palmer, A. *Acta Crystallogr. Sect. A* **1993**, 49, 590.

(14) Sakata, M. IUCr MEM project chairman, Department of Applied Physics, Nagoya University, Nagoya 464-01, Japan.

(15) Skilling, J. *Maximum Entropy and Bayesian Methods*; Skilling, J., Ed.; Kluwer Academic Publishers: Dordrecht, 1989; pp 46.

(16) Collins, D. M. *Nature* **1982**, *298*, 49.

(17) (a) Vries, R. Y.; Briels, W. J.; Feil, D. *Acta Crystallogr. Sect. A* **1993**, *50*, 383. (b) Iversen, B. B.; Nielsen, S. K.; Larsen, F. K. *Philos. Mag. A* **1995**, *72*, 1357.

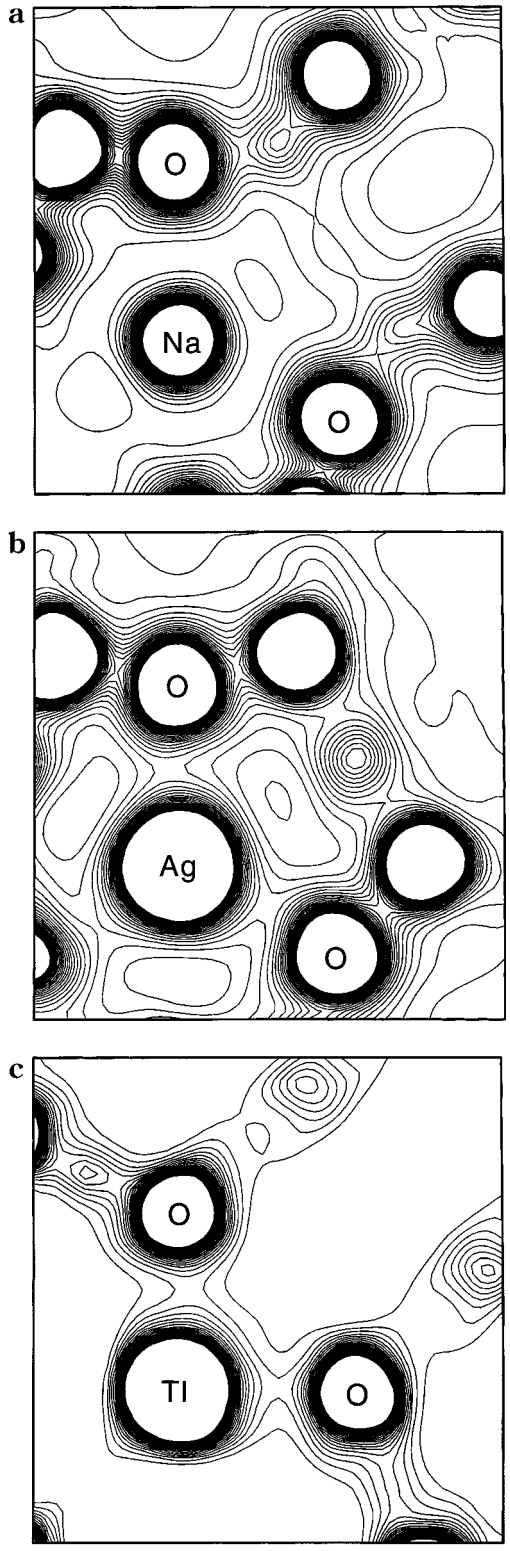

Figure 2. Contour plots of the (a) O−Na−O, (b) O−Ag−O, and (c) O−Tl−O planes. The contour interval is 1 e/Å^3. The plots are truncated at 25 e/Å^3, and the first contour is omitted.

heavy metal systems. Thus for NS the M−O distance exceeds the sum of ionic radii by 0.29 Å, whereas in AS and TS it is 0.24 and 0.15 Å shorter, respectively. The presumed covalent interaction in AS is further substantiated by the fact that AS undergoes a phase transition at high temperatures, which is related to the preference of silver ions to form three short bonds instead of six intermediate length bonds.[10d]

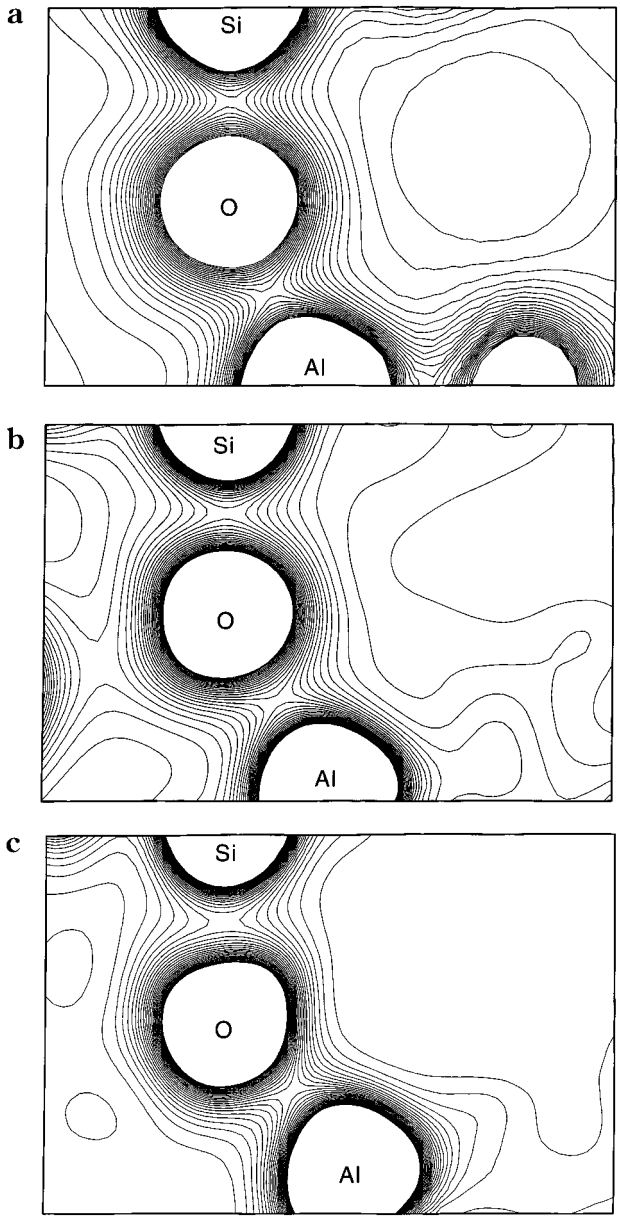

Figure 3. Contour plots of the Si−O−Al planes in (a) NS, (b) AS, and (c) TS. Contours as in Figure 2.

In Figure 2a−c, the O−M−O planes of the MEM electron densities are shown. These maps directly reveal the fundamental change in the framework−cation interaction when heavy metals are incorporated into the system. While the Na−O bond has little electron sharing and involves almost spherical atomic densities, the Ag−O and Tl−O bonds show directional character with electron density accumulation in the bonds. The effect is very pronounced for TS. In Figure 3a−c, Si−O−Al planes in the three structures are shown. The densities in the Si−O and the Al−O bonds are significantly higher than in the M−O bonds. Thus, even though the heavy metal to oxygen bonds show some covalency, they are still far from the covalency of the framework bonds. It must be stressed that the large changes in the host−guest bonding densities observed between NS and the heavy metal sodalites are evident in the MEM maps even though the temperature of the NS experiment is higher than in the AS and TS experiments (673 and 100 K, respectively). The high temperature means that the

NS density will be more affected by thermal smearing than the AS and TS densities. Thermal smearing will lower the features in the map, and thus the real differences in the interactions may be larger than what is revealed in the present maps. It should also be noted that due to the inherent thermal smearing of the MEM electron density map, it is difficult to quantitatively compare the MEM electron densities with static densities obtained from multipole modeling of single-crystal data.

The formation of partially covalent bonds to the guest species has a significant effect on the T−O framework bonds (T = Al or Si), and therefore also on spectroscopic observables such as ^{27}Al chemical shifts and quadrupole coupling constants (QCC). Considerable effort has been devoted to correlating parameters describing the asymmetry of the electron density around the Al site to chemical shifts or QCC values.[18] As shown in our related paper,[11] these correlations break down for AS and TS. The MEM densities provide an explanation for this. As seen in Figure 3a−c and Table 2, the formation of the partly covalent M−O bonds result in a decrease in the T−O bonding densities, but not in a simultanous structural distortion away from a tetrahedral environment. Theoretical calculations on zeolite acid sites predict that similar effects on the QCC are to be expected due to changes in the Al−O density when the acid site is protonated.[19]

3.2. Atomic Charges. One of the most definitive characterizations of molecular systems is based on topological analysis of the electron density.[2] Topological analysis requires calculation of not only the density itself, but also derivatives and second derivatives of the density. While this can be convincingly performed on multipole model densities,[20] it has only been successfully applied to the numerical MEM density of metallic beryllium, where very accurate single-crystal diffraction data exist.[13c] It has not been possible to obtain a meaningful topological analysis on the present MEM densities derived from synchrotron powder diffraction data. However, simpler and more robust methods of analysis can be performed. In Figure 4, integrated electron counts for spherical integration volumes around the framework atomic positions are plotted. The figure shows, as expected, that the Si sites in all three structures are more electron-rich than the Al sites. This demonstrates the physical soundness of the MEM densities. For TS a very large difference between the Si and Al sites is observed with the Al site being relatively depleted of electrons. In contrast to this the TS oxygen is relatively electron-rich. Overall the plot therefore demonstrates that heavy metal substitution leads to an electron flow from the Al site to the oxygen atom.

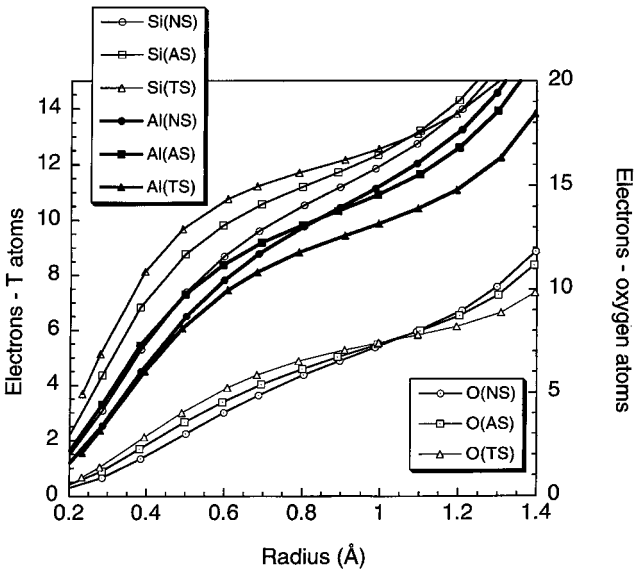

Figure 4. Electron counts for spherical integration volumes around the atomic positions.

Kurki-Suonio and Palmo suggested to use the minimum in the derivative of the spherical integration plots as a simple and fairly transferable definition of atomic radius.[21] The definition was found to be particularly good for ionic systems, and thus in the present case presumably best applied to the guest atoms. In parts a and b of Figure 5, derivative curves for all the atoms are shown. Figure 5a reveals that the atomic radii are similar for Si and Al in NS and AS, but that Al is slightly more diffuse than Si in TS. This supports that charge migration takes place from the Al site to the oxygen. This is further demonstrated in Figure 5b which shows that the oxygen atom in TS is expanded relative to the NS and AS structures. Across the series the Si radius varies by about 0.1 Å. This is probably not a real effect, and can instead be used as an indication of the reliability of the method.

In rationalization of aluminosilicate framework behavior, it is generally assumed that Al−O bonds are more ionic than the Si−O bond.[10b] The larger ionicity of the Al−O bond makes it more deformable than Si−O bonds, since there is less directional character in an electrostatic interaction. It is therefore observed that the AlO_4 tetrahedra generally adopt themselves to the situation in a given structure and that the framework conformation is mainly determined by the SiO_4 requirements.[10b] At the same time the larger ionic character of the Al−O bond makes it more polarizable, and since Al is also less electronegative than Si, electron density is more easily removed from the Al−O bond. The present study provides direct experimental validation for these assumptions, and the MEM analysis shows that when a covalent M−O bond is formed, it affects the Al−O density more than the Si−O density.

Figure 5b establishes the radii of the guest species, which presumably are better estimated than the framework atomic radii. The MEM density gives, as expected, an increasing atomic radius the heavier the metal with Na ∼1.25 Å, Ag ∼1.4 Å, and Tl ∼1.7 Å. For comparison

(18) (a) Engelhardt, G.; Koller, H.; Sieger, P.; Depmeier, W.; Samoson, A. *Solid State Nucl. Magn. Res.* **1992**, *1*, 127. (b) Kovalokova, M.; Grobet, P. J. *Solid State Nucl. Magn. Res.* **1997**, *9*, 107. (c) Engelhardt, G.; Veeman, W. *J. Chem. Soc. Chem. Comm.* **1993**, 622. (d) Nielsen, N. C.; Bildsoe, H.; Jakobsen, H. J.; Norby, P. *Zeolites* **1991**, *11*, 622.

(19) Koller, H.; Meijer, E. L.; van Santen, R. A. *Solid State Nucl. Magn. Reson.* **1997**, *9*, 165.

(20) Stewart, R. F. *Application of Charge Density research to Chemistry and Drug Design*; Jeffrey, G. A., J. F. Piniella, J. F., Eds.; Plenum Press: New York, 1991; p 63.

(21) Kurki-Suonio, K.; Salmo, P. *Ann. Acad. Sci. Fennicae* **1971**, *369*, 1.

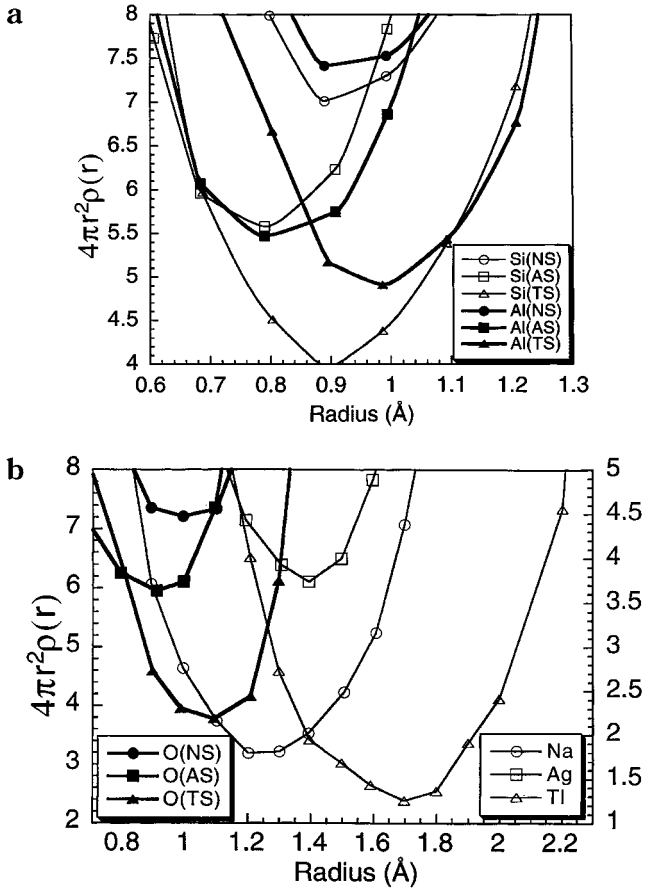

Figure 5. Derivative curves of spherical integration plots shown in Figure 4. Part a shows the Al and Si atoms, and part b, the O and M atoms. The minimum in these curves represents a simple and fairly transferable definition of atomic radii.

the atomic/ionic(+1) radii of the metals are Na(1.90/0.97 Å), Ag(1.44/1.26 Å), and Tl(1.60/1.47 Å). Simple chemical arguments about charge balancing in the sodalite structure generally assumes that the metal atoms have a single positive charge. This is because each substituted trivalent aluminum atom is thought to require an extra negative charge to fit into the tetrahedral framework. Such simple arguments are, however, sometimes at variance with the actual charge distributions in solids as found both experimentally and theoretically in for example thermoelectric clathrates.[22] The radii shown in Figure 5b supports that a fundamental change in the guest−host interaction occurs for AS and TS relative to NS. While the sodium charge appears to be slightly smaller than +1, the heavy metals appear closer to neutral.

There is a striking difference in thermal behavior between the alkali and the heavy metal sodalite systems. While NS goes through an order−disorder phase transition at 520 K,[12] AS and TS remain pseudo-cubic even at 100 K. The ordering of the sodium atoms is controlled by repulsive interactions between the cations.[12] However, the assumption of positive metal ions does not hold for AS and TS, and consequently the driving forces for ordering are reduced. At the same time

(22) Iversen, B. B.; Palmqvist, A. E. C.; Cox, D.; Nolas, G. S.; Stucky G. D.; Blake, N.; Metiu, H. *J. Solid State Chem.*, submitted for publication.

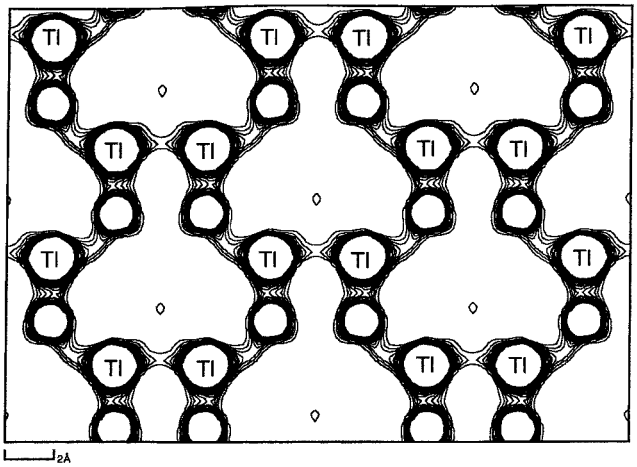

Figure 6. Contour plot in the very low-density regions of the [110] plane of TS. The plot shows four unit cells. The contour interval is 0.05 e/Å^3 and the plots are truncated at 1 e/Å^3.

the heavy metal atoms interact very strongly with the framework. Together these two properties of the charge distribution result in locked-in static disorders in AS and TS.

3.3. Thallium Cluster. The TS structure is of particular interest. Even though the structure has to incorporate very large atoms in the small β-cage, it is greatly contracted relative to NS and AS. Part of this may be due to the strong bonding to the framework, but this bonding is also present in AS. The structural parameters suggest that the cause of the contraction is the formation of a Tl cluster. In TS, the Tl−Tl distance is 3.734(2) Å, which is within the range found in organometallic materials where attractive Tl−Tl interactions have been suggested.[23] For thallium complexes with low coordination numbers, such as the Tl cluster in TS, it has qualitatively been suggested that the Tl 6s lone pair is stereoactive, a condition assumed to be present in for example TlF, Tl_3ThF_7, Tl_3VO_4, and $TlBePO_4$.[24] The common structural evidence for stereoactivity is low coordination numbers with typically three to four short bonds on one side of the Tl atom and very long secondary bonds, and the stereoactive lone pair, on the other side. On the basis of structural evidence this picture could easily be assigned to TS. However, the MEM electron density map shown in Figure 6 suggests that the center of the β-cage is of very low density (0.009 e/Å^3) in contradiction with the concept of stereoactive lone pairs. It should be stressed that the features of the MEM density in the very low density regions may not be reliable. Interpretation of these regions is therefore somewhat speculative. However, it may also be noted that even in the very low density

(23) (a) Hellmann, K. W.; Gade, L. H.; Scowen, I. J.; McPartlin, M. *J. Chem. Soc., Chem. Commun.* **1996**, 2515. (b) Hellmann, K. W.; Gade, L. H.; Fleischer, R.; Stalke, D. *J. Chem. Soc., Chem. Commun.* **1997**, 527. (c) Atencio, R.; Barbera, J.; Cativiela, C.; Lahoz, F. J.; Serrano, J. L.; Zurbano, M. M. *J. Am. Chem. Soc.* **1994**, *116*, 11558. (d) Jutzi, P.; Schnittger, J.; Hursthouse, M. B. *Chem. Ber.* **1991**, *124*, 1693. (e) Schumann, H.; Janiak, C.; Pickardt, J.; Borner, U. *Angew. Chem., Int. Ed. Engl.* **1987**, *26*, 789.

(24) (a) Gabuda, S. P.; Kozlova, S. G.; Davidovich, R. L. *Chem. Phys. Lett.* **1996**, *263*, 253. (b) Gaumet, V.; El-Ghozzi, M.; Avignant, D. *Eur. J. Solid State Inorg. Chem.* **1995**, *32*, 893. (c) Jouanneaux, A.; Joubert, O.; Fitch, A. N.; Ganne, M. *Mater. Res. Bull.* **1991**, *26*, 973. (d) Wallez, G.; Jaulmes, S.; Elfakir, A.; Quarton, M. *J. Solid State Chem.* **1995**, 114, 123.

regions of TS, there are only few spurious ghost features in the density. Weak attractions between Tl centers has in some cases been observed to determine the mode of molecular assembly in the solid state,[23] and the nature of the Tl−Tl interactions has been the subject of some debate. Extended Hückel calculations by Janiak and Hoffmann indicated formation of a weak covalent Tl−Tl bond in RTl−TlR dimers.[25] Unfortunately extended Hückel calculations are sometimes unreliable for heavy metal systems, and later ab initio calculations by Schwerdfeger questioned the presence of covalent bonding between the Tl atoms.[26] The MEM electron density suggests a small bridging bonding density between every pair of Tl atoms in the cluster. The electron density in these Tl−Tl bonds is low, but since the MEM density depicts the disordered structure with 0.75 occupancy on the metal sites, the true Tl−Tl covalent bonding density may be larger in magnitude.

(25) Janiak, C.; Hoffmanm, R. *J. Am. Chem. Soc.* **1990**, *112*, 5924.
(26) Schwerdfeger, P. *Inorg. Chem.* **1991**, *30*, 1660.

4. Conclusion

MEM electron density analysis has established that charge migration takes place from the framework, especially the Al site, to form covalent bonds to heavy metals such as Ag and Tl. The fundamental change in guest−host interactions relative to the more common alkali systems has a large effect on spectroscopic observables such as chemical shifts and QCC's. Simple chemical assumptions about the charge of the guest species are found to be less accurate for the heavy metal compounds, where the metals appear closer to neutral. The present study documents that chemically useful electron density information can be retrieved even from powder diffraction data.

Acknowledgment. The authors would like to thank Dr. Masaki Takata and Dr. Vojislav Srdanov for helpful discussions.

CM9910658